POLISH MARITIME RESEARCH 3 (123) 2024 Vol. 31; pp. 15-24
10.2478/pomr-2024-0032

Determination of Propeller-Rudder-Hull Interaction Coefficients in Ship Manoeuvring Prediction

Radosław Kołodziej*
Maritime Advanced Research Centre (CTO), Poland
Paweł Hoffmann
Maritime Advanced Research Centre (CTO), Poland

* Corresponding author: *radoslaw.kolodziej@cto.gda.pl (Radosław Kołodziej)*

ABSTRACT

The assessment of ship manoeuvring properties is a crucial part of the process of ship design and is usually first carried out during the model test phase of the project. According to the International Maritime Organisation (IMO), the manoeuvrability of the ship can be assessed on the basis of the standard trial manoeuvres. In order to do this, free running model tests or captive model tests are used, in conjunction with a mathematical model of ship motion; this is considered to be a reliable prediction method. In recent years, numerical-based methods have also been widely used in ship hydrodynamics and constantly improving computing power and more accurate fluid dynamics models have made the simulation of more complex cases possible. The study presented in this paper focuses on the determination of propeller-rudder-hull interaction coefficients based on the Mathematical Modelling Group (MMG) standard method in ship manoeuvring prediction. The identification of the parameters uses both captive model tests and a simplified numerical method, as well as regression formulas. The results of 35° turning and 10°/10° zig-zag manoeuvres, obtained with the use of each prediction method, are then compared. The test case used in the study is the container type cargo ship equipped with a single propeller and rudder. The model scale, for which the referenced model tests were carried out, is equal to 1:25 and a NACA 0020 rudder profile was used. This research highlights the advantages and disadvantages of each presented prediction method and their potential for future improvement.

Keywords: Ship manoeuvring model tests, Numerical manoeuvring tests, Ship manoeuvring prediction, MMG standard method, IMO standards for manoeuvring.

INTRODUCTION

The manoeuvring performance of a ship is one of the most crucial parameters when it comes to navigation safety. During the initial stages of ship design, the manoeuvrability of the ship is usually evaluated with the use of model tests. The prediction methods include empirical estimation, free running model tests and either captive model tests or virtual captive model tests, in conjunction with mathematical modelling of a ship's motion. A growing number of prediction methods require validation and, as a result, the international conference on ship manoeuvrability was organised in 2008 (SIMMAN 2008) [1]. The study included experimental benchmark data gathered from planar motion mechanism tests (PMM), circular motion tests (CMT), numerical simulations, and free running model tests. The researchers used different approaches to carry out the numerical simulations, which provided important reference data for manoeuvring simulations.

As of today, there are two mathematical models that are most often used. The first one was presented by Abkowitz [2] and considers the propeller, rudder and hull as a whole in motion equations. The second model was introduced by the MMG [3] and calculates the propeller, rudder and hull forces separately, with the inclusion of their mutual interactions. In both cases, the prediction accuracy depends on the accuracy of estimated hydrodynamic coefficients. The rapid development of software using Reynolds-Averaged Navier-Stokes Equations (RANSE) has resulted in a wider application of Computational

Fluid Dynamics (CFD) in manoeuvring prediction [4,5]. New methods based on artificial intelligence are also presented [6,7]. The studies aim to not only improve the prognosis accuracy but also reduce the number of necessary tests, in the search for a compromise between quality and efficiency.

The purpose of this research is to compare the manoeuvring predictions of cargo ships with propeller-rudder-hull interaction coefficients, based on the MMG method and obtained with captive model tests, virtual captive model tests and regression formulas. The presented virtual captive model tests include suggestions for a simplified testing procedure. Finally, the advantages and disadvantages of each estimation method are discussed.

MATHEMATICAL MODEL OF SHIP MOTION

MOTION EQUATIONS

The MMG model used in this study uses two corresponding coordinate systems. The forces acting on the ship are calculated with reference to a ship-fixed coordinate system located at the midship position (0,0,0), as presented in Fig. 1, with a centre of gravity of ship G located at (x_G,0,0).

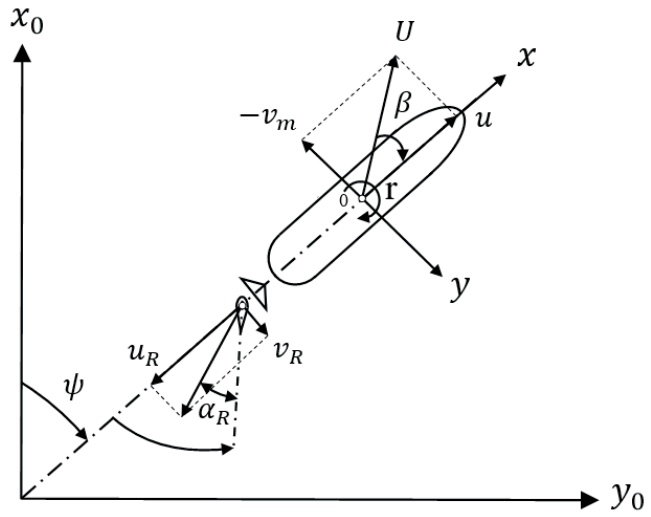

Fig. 1. Coordinate system

As a result, the following equations are obtained:

$$F_x = (m + m_x)\dot{u} - (m + m_y)v_m r - mx_G r^2 \quad (1)$$

$$F_y = (m + m_y)\dot{v}_m + (m + m_x)ur + mx_G\dot{r} \quad (2)$$

$$N_z = (I_{zG} + mx_G^2 + J_z)\dot{r} + mx_G(\dot{v}_m + ur) \quad (3)$$

$$v = v_m + x_G r \quad (4)$$

where m is the mass of the ship, v_m denotes the ship's lateral speed (midship), u is the longitudinal ship speed, r is the yaw rate, x_G is the longitudinal coordinate of the centre of gravity of the ship (calculated from midship), and I_{zG} is the moment of inertia of the ship around the centre of gravity. The m_x, my and J_z symbols stand for the added masses and added moment of inertia. The F_x, Fy and N_z symbols represent, in order, the surge and sway forces as well as the yaw moment acting on the ship, which are a sum of the following components:

$$F_x = X_H + X_P + X_R \quad (5)$$

$$F_y = Y_H + Y_R \quad (6)$$

$$N_z = N_H + N_R \quad (7)$$

The subscripts $_H$, $_R$ and $_P$ denote the forces and moments due to the hull, rudder and propeller, respectively. The ship-fixed coordinate system is later transformed back into an earth-fixed system for the assessment of ship manoeuvrability.

HULL FORCES

The forces acting on a hull during manoeuvring can be expressed, for practical purposes, in a non-dimensional form, as follows [1]:

$$X_H = 1/2\rho L_{PP} d U^2 X'_H(\beta, r') \quad (8)$$

$$Y_H = 1/2\rho L_{PP} d U^2 Y'_H(\beta, r') \quad (9)$$

$$N_H = 1/2\rho L_{PP}^2 d U^2 N'_H(\beta, r') \quad (10)$$

where ρ is the water density, L_{pp} is the length between perpendiculars, d stands for the ship draught and U is the ship velocity. The non-dimensional hull forces can now be expressed as polynomial functions using the drift angle β and $r' = rL_{pp}/U$:

$$X'_H = R_0' + X'_{\beta\beta}\beta^2 + X'_{\beta r}\beta r' + X'_{rr}r'^2 + X'_{\beta\beta\beta\beta}\beta^4 \quad (11)$$

$$Y'_H = Y'_\beta\beta + Y'_r r' + Y'_{\beta\beta\beta}\beta^3 + Y'_{rrr}r'^3 + (Y'_{\beta\beta r}\beta + Y'_{\beta rr}r')\beta r' \quad (12)$$

$$N'_H = N'_\beta\beta + N'_r r' + N'_{\beta\beta\beta}\beta^3 + N'_{rrr}r'^3 + (N'_{\beta\beta r}\beta + N'_{\beta rr}r')\beta r' \quad (13)$$

The polynomial coefficients in Eqs. 11, 12 and 13 are called 'hydrodynamic derivatives on manoeuvring'. There are various methods for assessing their value, including captive model tests and numerical simulations. It has to be pointed out that the presented polynomial coefficients include added masses.

PROPELLER FORCES

The surge force generated by a working propeller is expressed as:

$$X_P = (1 - t_P)\rho n_P^2 D_P^4 K_T \quad (14)$$

where t_p is the thrust deduction factor, ρ is the density of water, n_p represents the propeller revolutions and D_p is the propeller diameter. The propeller thrust open water efficiency K_T is a function of the propeller advance ratio coefficient J_P, which can be calculated as a fourth order polynomial function:

$$K_T = k_4 J_P^4 + k_3 J_P^3 + k_2 J_P^2 + k_1 J_P + k_0 \quad (15)$$

$$J_P = \frac{u(1-w_P)}{n_P D_P} \quad (16)$$

The inflow of water to the propeller changes considerably during manoeuvring because of the ship's drift angle. This phenomenon is difficult to capture and many algorithms have been proposed [3]. In this paper, the wake fraction coefficient of the propeller is calculated using the following formula, for simplicity [8]:

$$w_P = w_{P0} e^{-4\beta_P^2} \quad (17)$$

$$\beta_P = \beta - x'_P r' \quad (18)$$

RUDDER FORCES

The hydrodynamic forces induced by the rudder during manoeuvring can be calculated based on the rudder's normal force, according to the following equations:

$$X_R = -(1 - t_R)F_N \sin\delta \quad (19)$$

$$Y_R = -(1 + a_H)F_N \cos\delta \quad (20)$$

$$N_R = -(x_R + a_H x_H)F_N \cos\delta \quad (21)$$

where t_R is the steering resistance deduction factor, a_H is the rudder force increase factor, x_H is the longitudinal coordinate of the acting point of the additional lateral force and x_R is the longitudinal coordinate of the rudder position (usually, x_R = -0.5Lpp). The additional lateral force may be better understood when considering the ship and rudder relationship as the hydrodynamic interaction of a wing with a flap. The forces acting on the rudder are presented in Fig. 2.

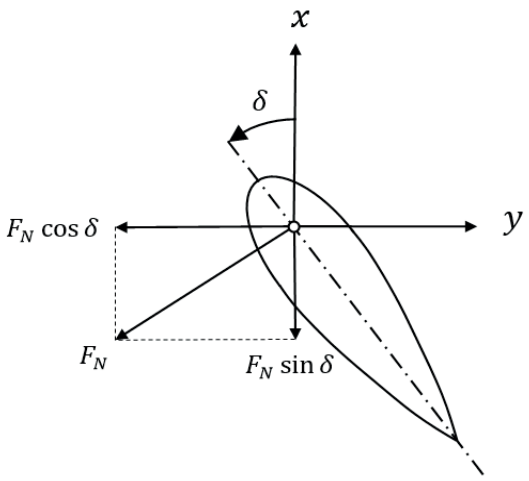

Fig. 2. Forces acting on the rudder

The rudder's normal force is expressed as:

$$F_N = 0.5\rho A_R f_a U_R^2 \sin\alpha_R \quad (22)$$

Here, A_R is the profile area of the moveable part of the rudder and f_a stands for the normal force coefficient:

$$f_a = \frac{6.13\Lambda}{2.25+\Lambda} \quad (23)$$

The Λ coefficient in Eq. (22) is equal to $\frac{h_R^2}{A_R}$, where h_R is the rudder span. The effective angle of the water inflow to the rudder α_R and the velocity of the water inflow to the rudder U_R are calculated according to:

$$\alpha_R = \delta - \tan^{-1}\frac{v_R}{u_R} \quad (24)$$

$$U_R = \sqrt{u_R^2 + v_R^2} \quad (25)$$

The components of the water inflow to the rudder velocity are calculated based on the results of experiments. The lateral velocity to the rudder is equal to:

$$v_R = U\gamma_{R\pm}(\beta - r'l'_R) \quad (26)$$

The $\gamma_{R\pm}$ value in Eq. (26) is the flow straightening coefficient and l'_R is the effective longitudinal coordinate of the rudder position. The $'$ symbol stands for non-dimensional values. The longitudinal component of rudder inflow velocity u_R consists of the sum of velocities where the propeller slip stream hits u_{RP} and where it does not, u_{R0}. Additionally, it is assumed that:

$$\eta = \frac{A_{RP}}{A_R} \cong \frac{D_P}{H_R} \quad (27)$$

where A_{RP} is the rudder area when the slip stream hits and A_R is the total projected lateral rudder area. The inflow velocity u_R is equal to:

$$u_R = \sqrt{\eta u_{RP}^2 + (1-\eta)u_{R0}^2} \quad (28)$$

The u_{RP} can now be expressed by introducing the rudder wake fraction coefficient, which represents water velocity at the rudder position without a working propeller:

$$u_{RP} = (1 - w_R)u + k_x \Delta u \quad (29)$$

The $k_x \Delta u$ value in Eq. (29) is a theoretical velocity increase due to a propeller with a correction factor. By expressing propeller thrust T as the pressure difference between the aft and fore of the propeller disc (Eq. (30)) and combining it with Bernoulli's theorem in Eq. (31):

$$\rho n_P^2 D_P^4 K_T = \Delta p \frac{1}{4}\pi D_P^2 \quad (30)$$

$$\Delta p + \frac{\rho}{2}u_P^2 = \frac{\rho}{2}u_R^2 \quad (31)$$

The following equation for the longitudinal component of rudder inflow velocity u_R is obtained:

(32)

The κ value in Eq. (32) is an experimental constant, which can be written as [3,9]:

$$u_R = (1 - w_P)u\varepsilon\sqrt{\eta\left\{1 + \kappa\left(\sqrt{1 + \frac{8K_T}{\pi J_P^2}} - 1\right)\right\}^2 + (1-\eta)} \quad (33)$$

The ε value in Eq. (32) represents the ratio of wake fraction coefficients in the rudder and propeller position and is established experimentally. It has to be pointed out that, by using the classical MMG method, ε is also influenced by the rudder profile effect when using classical equations for normal force coefficient f_a.

$$\varepsilon = \frac{(1-w_R)}{(1-w_P)} \quad (34)$$

INVESTIGATED CASE

The test case used in this study was the container type cargo ship designed by the Nelton Sp. z o.o. company. The ship is equipped with a single left-handed propeller. The model scale, at which the model tests were carried out, was equal to 1:25 and the NACA 0020 rudder profile was used during the tests. The numerical captive model tests presented were also undertaken at model scale, in order to simplify the computing domain. The model metacentric height (GM) was large enough that the roll coupling effect on manoeuvring was considered to be negligible. The hull model and stock propeller were manufactured in accordance with the requirements given in the following ITTC Recommended Procedures [10,11]. Table 1 presents the basic model parameters and the ship model is presented in Fig. 3.

Tab. 1. Parameters of tested ship

	Symbol	Unit	Real scale	Model scale
Scale	λ	[-]	1:1	1:25
Length between perpendiculars	L_{PP}	[m]	155.4	6.22
Breadth at waterline	B	[m]	26.6	1.06
Draught	d	[m]	8.1	0.32
Block coefficient	C_B	[-]	0.64	
Longitudinal coordinate of the centre of gravity from midship	x_G	[m]	-1.5	-0.06
Radius of the gyration of the ship around the centre of gravity (related to Lpp)	k'_{yy}	[-]	0.25	
Propeller diameter	D_P	[m]	5.8	0.23
Propeller direction of rotation	-	-	counter-clockwise	
Rudder projected lateral moveable area	A_R	[m2]	25	0.04
Rudder height	h_R	[m]	5.8	0.23
Rudder turn rate	-	[°/s]	11.6	2.32

Fig. 3. Container type cargo ship tested

CAPTIVE MODEL TESTS

The captive model tests were conducted at the Maritime Advanced Research Centre (CTO S.A.) with the use of PMM. The model speed U_0 was set at 1.646 m/s (equivalent to 16.0 kn at full scale). After that, the following tests were conducted:

- Rudder force test in the straight, moving under different rudder angles (propeller revolutions n_p = 9.3 rps).
- Rudder force test in the straight, moving under various propeller loads (propeller revolutions n_p = 7.8, 8.5, 8.7, and 9.3 rps).
- Rudder force test in oblique towing (propeller revolutions n_p = 9.3 rps).

During the tests, both the hull surge and rudder surge were measured, as well as the lateral forces, the yaw moment around the midship, and the propeller thrust. The tests were carried out in the free condition for trim and signage of the model. The test apparatus consisted of a propulsion dynamometer, rudder dynamometer and hull dynamometer. The yaw moment was captured by the measurement of two lateral hull forces. The methods used to carry out the testing followed the methodology given in the IMO documents [12,13] and the ITTC Recommended Procedure for captive model tests [14]. Measurement uncertainty in the presented method is discussed in the related ITTC procedure [15]. The measuring accuracy of each dynamometer component is presented in Table 2 and the results of the tests are presented in Fig. 7.

Tab. 2. Measurement accuracy of dynamometers

Measurement uncertainty for 0.95 confidence level					
Propeller thrust	Rudder X force	Rudder Y force	Hull X force	Hull fore Y force	Hull aft Y force
± 0.11N	± 0.34N	± 0.37N	± 0.25N	± 1.31N	± 1.34N

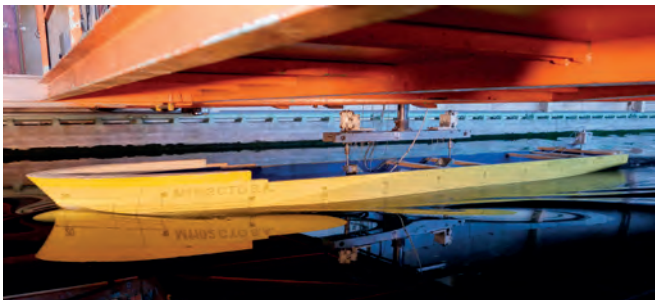

Fig. 4. Captive model tests with the use of PMM

VIRTUAL CAPTIVE MODEL TESTS

The CFD simulations were conducted at a model scale using the RANSE method. The mesh creation and the calculations were conducted using Simens Simcentre (STAR-CCM+). The solving methods used in the computation followed ITTC guidelines [16] and are listed below:

- Rigid Body Motion: governs the movement of the propeller and moves the vertices of the rigid grid according to a prescribed formula.
- Volume Of Fluid: an interface-capturing method that predicts the distribution and the movement of the interface of immiscible phases. The High Resolution Interface Capturing scheme was used.
- k-omega SST turbulence: a two-equation model that solves transport equations for the turbulent kinetic energy and the specific dissipation rate in order to determine the turbulent flow conditions. The SST turbulence model combines the advantages of k-omega and k-epsilon models using a blending function that allows good accuracy in the boundary layer region (k-omega) and better performance in free stream regions (k-epsilon). This turbulence model was successfully implemented in the determination of propeller-hull interaction coefficients in other studies [17,18].
- The 'All y+' wall treatment was used for modelling near-wall turbulence quantities.
- The solution was assumed to reach convergence when the fluctuation of the forces monitored on the hull and the rudder were stable for at least 15 seconds of simulated time.

The use of the above-mentioned model allowed better capture of the turbulent flow near the propeller and the rudder and, at the same time, the general flow around the hull was simulated with good accuracy. The computational mesh was divided into two distinct parts, similar to other studies on propellers [19]: the rotating cylinder with the propeller inside and a stationary region containing the ship, the rudder and the rest of the volume around it. The time step used in the calculations was set to 0.001 s at the final phase of calculations. 0.05 s was used in the initial time period and this was small enough so that its impact was insignificant. The propeller was meshed with polyhedral cells and the stationary domain was meshed using hexahedral cells; the number of elements was 450.000 and 2 million, respectively. The domain size was 40 × 26 × 12 m with the model's midship located at its centre. The 3D meshes and computational domain are presented in Fig. 5 and Fig. 6.

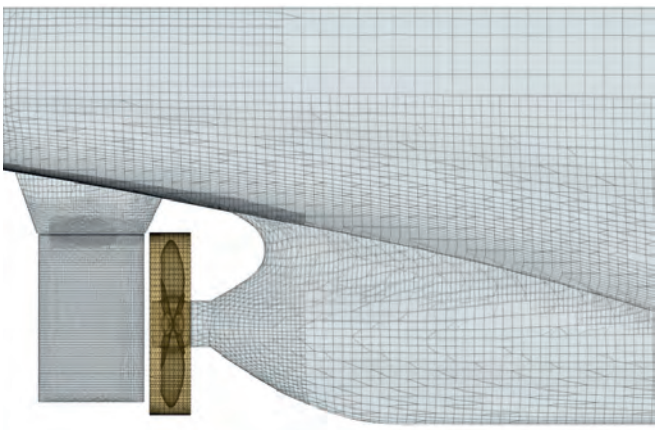

Fig. 5. Virtual captive model tests – 3D mesh

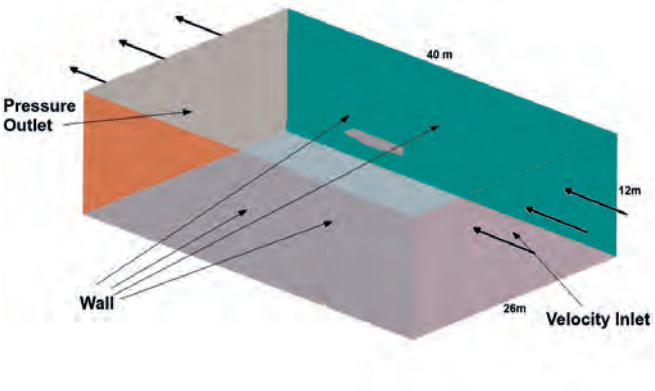

Fig. 6. Virtual captive model tests – computational domain

Prior to the simulations, a mesh sensitivity study was conducted in the case of a rudder deflection of 0°. The computational meshes were generated in sequence, where every next mesh had the number of the cells doubled. Despite the cell count doubling, the values of the considered parameters changed very little between subsequent meshes, which proved good convergence (as presented in Fig. 7). The mesh used for the manoeuvring simulations is shown in red. The verification and validation of the numerical model was carried out according to the ITTC procedure [20].

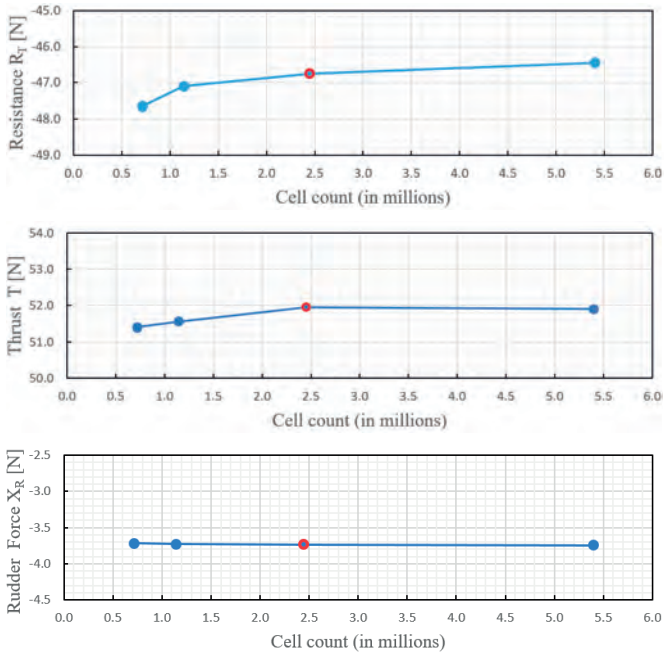

Fig. 7. Mesh sensitivity study

RESULTS OF CAPTIVE TESTS

The resulting forces and moments obtained by the numerical rudder force tests, at different rudder angles, generally showed good agreement with the model tests, having slightly higher values. What is more, it should be noted that, for higher rudder angles, the normal force F_N drops in the case of model tests, which has no place during numerical tests. As this effect is not expected to take place for a drifting hull, those points were not taken into consideration in the analyses. The propeller thrust measured with both methods showed an increasing trend with rudder deflection, which is equal to about 15% in the case of maximum rudder angle. This leads to the conclusion that either the thrust deduction factor or the wake fraction coefficient may not have a constant value with rudder deflection, and this requires further study. The results of the rudder force tests at different rudder angles are presented in Fig. 8.

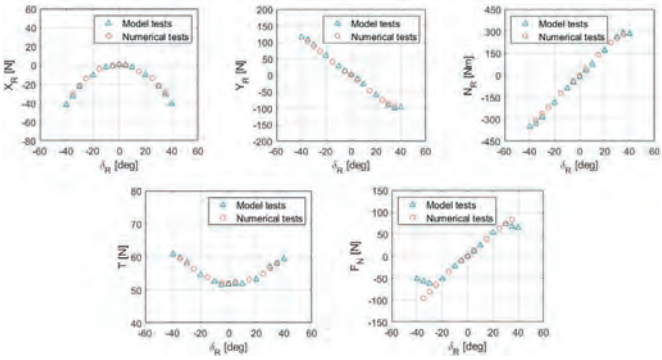

Fig. 8. Results of rudder force tests with different rudder angles

Rudder force tests in the straight, moving under various propeller loads, were carried out in order to estimate the water acceleration at the rudder position. The tests were performed with the use of model tests at four propeller loads and a non-deflected rudder. The interaction coefficient ε represents the ratio of wake fraction at the propeller disc to the wake fraction at the rudder position and was determined based on the measurement of the rudder's normal force F_{N0} (Fig. 10). In the case of the numerical version of the test, direct measurement of the water velocity near the propeller plane and rudder was carried out in order to reduce the number of necessary simulations, since $\eta \cong 1$ for the tested ship (see Fig. 9). The ratio was calculated as the average value in the area equal to the propeller diameter.

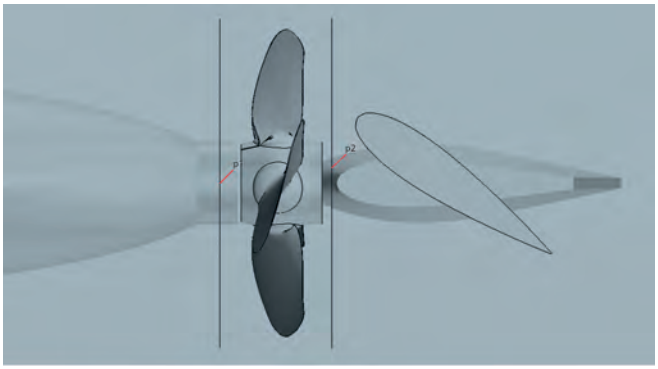

Fig. 9. Numerical determination of water velocity at propeller and rudder position

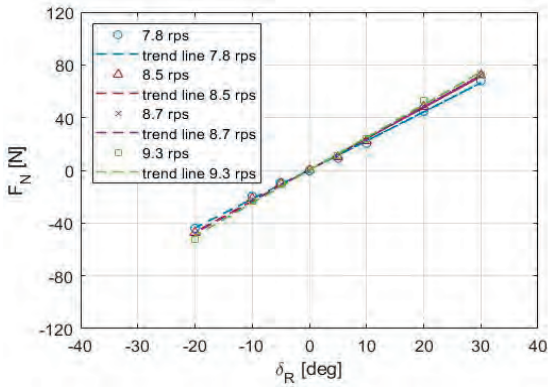

Fig. 10. Rudder force test in the straight moving under various propeller loads

The rudder force test under oblique towing was carried out in order to determine the flow straightening coefficients $\gamma_{R\pm}$. The tests were conducted for various drift angles and a non-deflected rudder. The coefficients for starboard and portside turning were calculated through the measurement of rudder normal forces – F_{N0}. The results of the tests presented in Fig. 11 show that the rudder normal force obtained with numerical methods is larger.

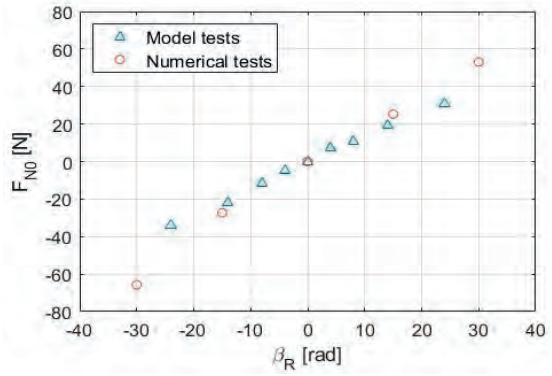

Fig. 11. Rudder force test in oblique towing

The effective longitudinal position of the rudder was only calculated with numerical methods because the model tests could not have been performed because of measuring range limitations. The coefficient l'_R is determined by the measurement of the rudder normal force F_{N0} of the non-deflected rudder at different rates of turn. Since the relation between rudder lateral velocity and rate of turn in this test is linear, it was decided that turning to one side was sufficient, thus limiting the number of tests. The results of the simulations are presented in Fig. 12.

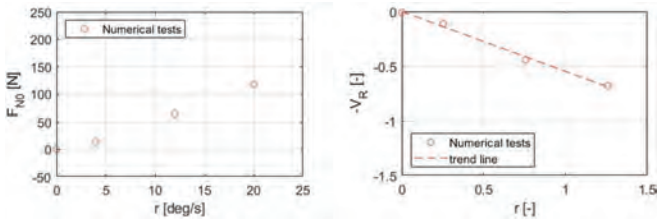

Fig. 12. Estimation of effective longitudinal rudder position

PROPELLER-RUDDER-HULL INTERACTION COEFFICIENTS

The interaction coefficients represent the relation between each ship component: the rudder, hull and propeller. Yasukawa and Yoshimura [3] confirmed that the interaction between the rudder and hull forces can be approximated with the linear function for a given propeller load. The results of the model tests and the numerical simulations in rudder force tests are a good match, the results obtained with the variable load tests and direct measurements of water velocity near the propeller and rudder positions gave similar results, so they are in good agreement, from a simulation perspective. The forces measured during oblique towing differ significantly between the model tests and numerical simulations and are larger in the case of CFD tests. The comparison of the force measurements, using captive model tests and virtual captive model tests, is presented in Fig. 13.

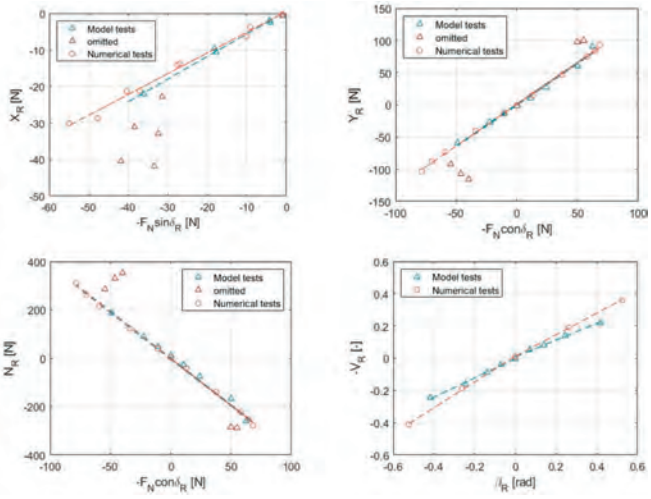

Fig. 13. Determination of propeller-rudder-hull interaction coefficients

The results of each propeller-rudder-hull interaction coefficient acquired with captive model tests and numerical methods are put together with the regression formulas for merchant vessels (suggested by Yoshimura and Masumoto [9]) and included in Table 3. It should be noted that the rudder-hull interaction coefficients t_R, a_H, x'_H, as well as the ratio of wake fractions ε, are similar for model and numerical tests, with the regression formula having a larger error. The flow straightening coefficients differ considerably for each estimation method in the cases of both the averaged and the portside and starboard values. The difference in values between portside and starboard is different for the model and numerical tests, the latter showing larger asymmetry. The effective longitudinal rudder position varies a little between the regression formula and CFD.

Tab. 3. Parameters of tested ship

Model tests							
t_R	a_H	x'_H	ε	k_x	γ_R^+	γ_R^-	l'_R
0.277	0.292	-0.412	1.140	0.55	0.52	0.60	-
Numerical tests							
t_R	a_H	x'_H	ε	k_x	γ_R^+	γ_R^-	l'_R
0.334	0.293	-0.414	1.158	0.55	0.67	0.80	-0.82
Regression formula							
t_R	a_H	x_H	ε	k_x	γ_R		l'_R
0.390	0.392	-0.400	1.108	0.55	0.364		-0.90

SHIP MANOEUVRING PREDICTION

In order to perform the manoeuvring prediction, using the mathematical model of ship motion presented by the MMG, the following parameters must be known:

- Ship model resistance (R_0).
- Propeller open water characteristics.
- Effective wake and thrust deduction coefficients, obtained through propulsion tests (w_p, t_p).
- Added mass coefficients for surge and sway motions and yaw moment (m_x, m_y, J_z).
- Hydrodynamic hull derivatives (x′, y′, n′).
- Propeller-rudder-hull interaction coefficients.

In this study, model resistance, self-propulsion and propeller open water tests were carried out in advance. The added mass coefficients were calculated using Hooft's and Pieffers' formulas [21] and hull hydrodynamic coefficients were obtained with the virtual CMT, according to the method presented by Kołodziej and Hoffmann [22]. The parameters used in the manoeuvring simulations are presented in Table 4.

Tab. 4. Parameters used in simulations.

R'_0	-0.01490	n'_b	0.06875
x'_{bb}	-0.005272	n'_{bbb}	-0.20230
x'_{bbbb}	0.77760	n'_{bbr}	-0.13670
x'_{br}	-0.08195	n'_{rr}	-0.03422
x'_{rr}	-0.01078	n'_r	-0.02331
y'_b	0.18040	n'_{rrr}	-0.01151
y'_{bbb}	0.79600	w_P	0.36700
y'_{bbr}	-0.05040	t_P	0.25500
y'_{brr}	0.21070	m'_x	0.01870
y'_r	0.05170	m'_y	0.14430
y'_{rrr}	0.01329	J'_z	0.00480

The simulation of ship manoeuvrability was carried out for 35° turning manoeuvres, as well as 10°/10° zig-zag tests. The rudder steering rate and propeller revolutions were equal to 11.6 °/s and 9.3 rps. The simulations were run using @MATLAB Simulink software with the ODE 4 solver and a constant 0.01 s time step (i.e. small enough that the solver impact was marginal from a practical perspective). The results of the turning circles are presented in Fig. 14 and zig-zag manoeuvres are presented in Fig. 15. The IMO criteria parameters obtained for ship manoeuvrability are presented in Table 5. The results of simulated turning circles show considerable differences between each presented method of estimation. In general, the turning results based on coefficients obtained with numerical methods overestimates IMO criteria for turning compared to model tests. The regression method underestimates these criteria.

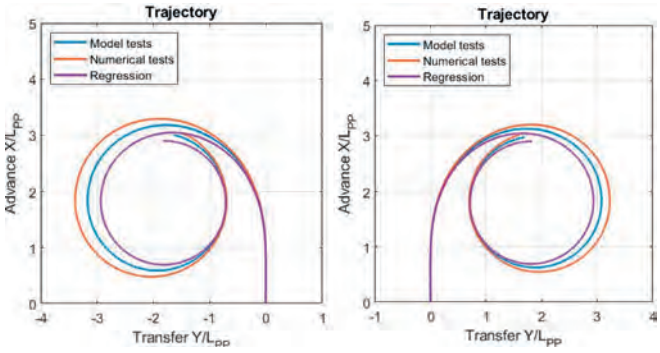

Fig. 14. Comparison of simulated 35° turning manoeuvres

The results of simulated zig-zag manoeuvres are also considerably different for each estimation method. The prognosis made with the use of numerical tools underestimates overshot angles (OSA) and overestimates initial turning ability over time (t'_A) when compared to the model tests. The simulated zig-zag manoeuvres, based on the coefficient obtained with regression formulas, have a contrary trend to the numerical tests.

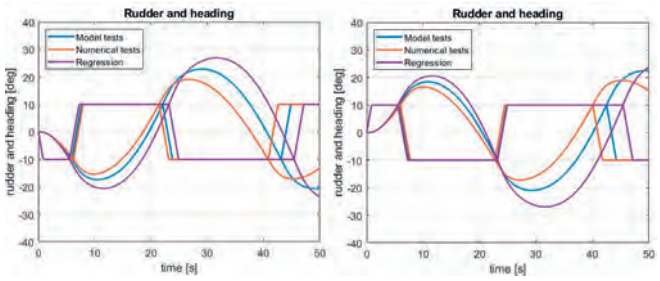

Fig. 15. Comparison of simulated 10°/10° zig-zag manoeuvres

Tab. 5. IMO criteria parameters obtained

Model tests					
	Advance	Tactical diameter	1st OSA	2nd OSA	t'_A
Starboard	2.97	2.94	8.4°	10.9°	1.52
Portside	3.02	3.03	7.4°	12.8°	1.56
Numerical tests					
	Advance	Tactical diameter	1st OSA	2nd OSA	t'_A
Starboad	3.05	3.09	6.5°	7.3°	1.58
Portside	3.14	3.26	5.3°	9.1°	1.65

Regression					
	Advance	Tactical diameter	1st OSA	2nd OSA	t'_A
Starboard	2.88	2.79	10.6°	16.9°	1.46
Portside	2.88	2.79	10.6°	16.9°	1.46
Numerical tests / Model tests					
Starboard	1.03	1.05	0.77	0.67	1.04
Portside	1.04	1.08	0.72	0.71	1.06
Regression / Model tests					
Starboard	0.97	0.95	1.26	1.55	0.96
Portside	0.95	0.92	1.43	1.32	0.94

CONCLUSIONS

This study presents a numerical approach to the determination of the propeller-rudder-hull interaction coefficients using the MMG standard method. The calculations were validated by the measurements carried out with the use of classical captive model tests. Next, both methods, together with regression formulas, were implemented to estimate IMO standard manoeuvres and the results were compared. The presented CFD simulations used the K-ω SST turbulence model because of its universal quality.

The study showed good correlation of the measured forces between model tests and virtual model tests in the rudder force test. Both methods captured thrust increase with rudder deflection, which leads to the conclusion that it influences propulsion coefficients. This phenomenon is not taken into consideration in the presented manoeuvring model and will be studied further.

The results proved that the CFD tools can be successfully implemented in the determination of rudder-hull interaction coefficients. A simplified numerical method also provided satisfying results in the case of the wake fraction ratio and the effective longitudinal rudder position, but highly overestimated the flow-straightening coefficients responsible for the asymmetry between starboard and portside manoeuvres. This is believed to be the reason for the general overestimation of IMO criteria parameters in the case of turning manoeuvres and initial turning ability times, as well as the underestimation of overshoot angles in the case of zig-zag manoeuvres. The correct approach to estimating flow-straightening coefficients using CFD requires additional study.

Direct measurement of water inflow velocity to the rudder was undertaken because the propeller slip stream speed u_{RP} is the only component of rudder speed u_R in the case of the investigated ship. Additional study is necessary for this type of measurement for smaller η ratios and different rudder types.

The use of regression formulas in manoeuvring prognosis is the least time consuming but less accurate method, which benefits from the already gathered reference data and experience of the user. Despite that, this method might provide a good means for reducing the number of numerical simulations necessary for obtaining hydrodynamic coefficients of MMG models. For example, calculating flow-straightening coefficients with such formulas would enable the use of an accelerating disk in place of a propeller model, thus simplifying the preparation phase of simulations and reducing the number of tests. This approach will be studied in the future.

Numerical methods show a lot of potential in ship manoeuvring prediction because they do not require the production of a model or the usage of special measuring devices, which makes them more flexible than traditional model tests. As mentioned, the practical engineering aspect requires the prognosis method to not only be accurate but also effective. In order to meet this demand, future studies will focus on not just improving mathematical and numerical models but also on combining the presented prediction methods.

ACKNOWLEDGEMENTS

This manuscript was undertaken within the framework of the internal research of the Maritime Advanced Research Centre (CTO S.A.) in 2023.

©2024 The MathWorks, Inc. MATLAB, and Simulink are registered trademarks of The MathWorks, Inc. See *mathworks.com/trademarks* for a list of additional trademarks.

Computations were carried out using the computers at the Centre of Informatics Tricity Academic Supercomputer and network.

The research will be partially presented during the 2024 ISOPE conference and abstract.

The authors would like to express gratitude to Nekton Sp. z o.o company for their support in the preparation of this study.

REFERENCES

1. Yoshimura Y, Ueno M, Tsukada Y. Analysis of steady hydrodynamic force components and prediction of manoeuvring ship motion with KVLCC1, KVLCC2 and KCS. Workshop on verification and validation of ship manoeuvring simulation method, Workshop Proceedings, vol. 1, Copenhagen, pp. E80–E86, SIMMAN 2008.

2. Abkowitz MA, Liu G. Measurement of ship resistance, powering and manoeuvring coefficients from simple trials during a regular voyage. Trans SNAME 96, pp. 97–128, 1988.

3. Yasukawa H, Yoshimura Y. Introduction of MMG standard method for ship manoeuvring predictions. Journal of Marine Science and Technology, Japan, 2015. (DOI: 10.1007/s00773-014-0293-y).

4. Dai K, Li Y. Manoeuvring prediction of KVLCC2 with hydrodynamic derivatives generated by a virtual captive test. Polish Maritime Research 4 (104), Vol. 26, pp. 16-26, Poland, 2019. (DOI: 10.2478/pomr-2019-0062).

5. Sadati K, Zeraatgar K, Moghaddas A. Simulation of turning manoeuvre of planing craft taking into account the running attitude change in a simplified manner. Polish Maritime Research 4 (116), Vol. 29, pp. 12-25, Poland, 2022. (DOI: 10.2478/pomr-2022-0040).

6. Mei B, Sun L, Shi G, Liu X. Ship manoeuvring prediction using grey box framework via adaptive RM-SVM with minor rudder. Polish Maritime Research 3 (103), Vol. 26, pp. 115-127, Poland, 2019. (DOI: 10.2478/pomr-2019-0052).

7. Yoon HK, Rhee KP. Identification of hydrodynamic coefficients in ship manoeuvring equations of motion by Estimation-Before-Modelling technique. Ocean Engineering, Volume 30, Issue 18, pp. 2379-2404, 2003. (DOI: 10.1016/S0029-8018(03)00106-9)

8. Lee H, Shin S. The prediction of ship's manoeuvring performance in initial design stage. Hyundai Maritime Research Institute, Elsevier Science B.V., 1998. (DOI: 10.1016/s0928-2009(98)80205-9).

9. Yoshimura Y, Masumoto Y. Hydrodynamic Database and Manoeuvring Prediction Method with Medium and High-Speed Merchant Ships and Fishing Vessels. MARSIM, 2012.

10. 28th International Towing Tank Conference. Ships Models. Procedure 7.5-01-01-01 Revision 04, 2017.

11. 28th International Towing Tank Conference. Propeller Model Accuracy. Procedure 7.5-01-02-02 Revision 01, 2017.

12. International Maritime Organisation. Standards for Ship Manoeuvrability. Resolution MSC.137(76), London, 2002.

13. International Maritime Organisation. Explanatory Notes to the Standards for Ship Manoeuvrability. MSC/Circ. 1053, London, 2002.

14. Manoeuvring Committee of 28th International Towing Tank Conference. Captive Model Tests. Procedure 7.5-02-06-02 Revision 05, 2017.

15. Manoeuvring Committee of 28th International Towing Tank Conference. Uncertainty Analysis for Manoeuvring Predictions based on Captive Manoeuvring Tests. Procedure 7.5-02-06-04 Revision 05, 2017.

16. 28th International Towing Tank Conference. Guideline on Use of RANS Tools for Manoeuvring Prediction. Procedure 7.5-03-04-01 Revision 01, 2017.

17. Shang H, Zhan C, Liu Z. Numerical Simulation of Ship through Self-Propulsion. Journal of Marine Science and Engineering, Volume 9, Issue 9, 2021. (DOI: 10.3390/jmse9091017).

18. Zinati A, Ketabdari MJ, Zeraatgar H. Effects of Propeller Fouling on the Hydrodynamic Performance of a Marine Propeller. Polish Maritime Research 1 (117), Vol. 30, pp. 61-73, Poland, 2023. (DOI: 10.2478/pomr-2023-0059).

19. Ngoc TT, Luu DD, Nguyen THH, Nguyen TTQ, Nguyen MV. Numerical Prediction of Propeller-Hull Interaction Characteristics Using RANS Method. Polish Maritime Research 2 (102), Vol. 26, pp. 163-172, Poland, 2019. (DOI: 10.2478/pomr-2019-0036).

20. 28th International Towing Tank Conference. Validation and Verification of RANS Solutions in the Prediction of Manoeuvring Capabilities. Procedure 7.5-03-04-02 Revision 01, 2017.

21. Hooft JP, Pieffers J. Manoeuvrability of frigates in waves. Marine Technology, vol. 25, no. 4, pp. 262–271, 1988. (DOI: 10.5957/mt1.1988.25.4.262).

22. Kołodziej R, Hoffmann P. Numerical Estimation of Hull Hydrodynamic Derivatives in Ship Manoeuvring Prediction. Polish Maritime Research 2 (110), Vol. 28, pp. 46-53, Poland, 2021. (DOI: 10.2478/pomr-2021-0020).